Journal of Materials Chemistry A

RSC Publishing

PAPER

View Article Online
View Journal | View Issue

Cite this: J. Mater. Chem. A, 2013, 1, 10142

Enhancing the open circuit voltage of dye sensitized solar cells by surface engineering of silica particles in a gel electrolyte

Lioz Etgar,*[ab] Guillaume Schuchardt,[b] Daniele Costenaro,[c] Fabio Carniato,[c] Chiara Bisio,[c] Shaik M. Zakeeruddin,[b] Mohammad K. Nazeeruddin,[b] Leonardo Marchese[c] and Michael Graetzel[b]

Received 10th April 2013
Accepted 20th June 2013

DOI: 10.1039/c3ta11436h

www.rsc.org/MaterialsA

We prepared a quasi-solid electrolyte for dye-sensitized solar cells (DSSCs) that consist of ionic liquid and modified silica particles. Commercial bare silica F5 particles and modified silica F5 by NH_2 and NH_3^+ groups were prepared, and fully characterized. The best photovoltaic performance was observed using the NH_2 modified silica particles giving an open circuit voltage (V_{oc}) of 815 mV, a short-circuit current (J_{sc}) of 11.23 mA cm^{-2}, and a fill factor (FF) of 0.75 corresponding to an overall power conversion efficiency of 7.04% at 100 mW cm^{-2} AM 1.5. The modification of the silica particles by NH_2 groups increases the V_{oc} of DSSCs by around 60 mV compared to pure ionic liquid electrolyte based DSSCs.

Introduction

Dye-Sensitized Solar Cells (DSSCs) are directly inspired by photosynthesis present in plants, and are promising photovoltaic devices, because of their low cost and high efficiency.[1] The DSSC differs widely from conventional silicon-based solar cells, where the light absorption, charge separation and charge transport are carried out by different components. Its colour, lightweight architecture affords much greater flexibility in terms of integration into emerging technologies and it offers much promise in the field of sustainable energy solutions. The DSSC consists of a TiO_2 layer, deposited on FTO glass, coated with a dye and immersed in a liquid electrolyte, which contains a redox couple, usually I^-/I_3^-.[2,3] The liquid electrolyte in the cell presents several problems such as solvent evaporation, leakage and penetration of air and water caused by difficulty in long-term sealing and in temperature cyclic tests.

In order to overcome these problems several attempts were made to quasi-solidify the liquid electrolyte by using polymer matrices[4–7] or p-type semiconductors[8–11] or organic hole transport materials.[12–16] The main problem in these cases was the difficulty of filling the nanosized pores of the electrode, which results in insufficient conversion efficiencies of the solid cells compared to those using liquid electrolytes. To solve this problem, scientists have focused on quasi-solid electrolytes incorporating SiO_2 nanoparticles[17] and small molecular organogels.[18–20] The addition of nanoparticles to liquid electrolytes forms a viscous gel electrolyte and reduces the fluidity compared to liquid electrolytes. DSSCs using a quasi-solid electrolyte incorporating spherical type inorganic nanoparticles yielded 7% efficiency at AM 1.5 sunlight.[21,22] The inorganic nanoparticles employed in these systems have no direct role in the increment of light harvesting efficiency. Tu *et al.* used a polymer/montmorillonite nanocomposite by emulsion polymerization and applied it to a gel electrolyte system for DSSCs. Electrochemical impedance analysis revealed that the nanocomposite-gelled electrolyte had a significantly decreased resistance.[23]

In this study, quasi-solid electrolytes for DSSCs were prepared using unmodified SiO_2 particles and organo-modified silica samples functionalized with $-NH_2$ or $-NH_3^+$ groups. The preparation and characterization of the modified silica particles are presented; in addition, photovoltaic characterization reveals that the device's open circuit voltage increase depends on the modification. In the case of the NH_2 modified silica particles the open circuit voltage increased by $\approx$62 mV, which can be a result of pH changing and inhibition of the recombination rate.

Experimental

2.1 Materials preparation

1.00 g of amorphous silica F5 (Akzo-Nobel) was treated in a vacuum at 200 °C for 2 h, aiming at removing physisorbed water. After the treatment, the sample was kept under N_2 flow and then dispersed in 100 mL of toluene. 0.53 mL of 3-aminopropyltriethoxysilane were then added drop by drop to the

[a]Institute of Chemistry, The Hebrew University of Jerusalem, Jerusalem 91904, Israel. E-mail: lioz.etgar@mail.huji.ac.il

[b]Laboratoire de Photonique et Interfaces, Institut des Sciences et Ingénierie Chimiques, Ecole Polytechnique Fédérale de Lausanne, Station 6, CH-1015 Lausanne, Switzerland

[c]Dipartimento di Scienze e Innovazione Tecnologica and Nano-SISTEMI Interdisciplinary Centre, Università del Piemonte Orientale "A. Avogadro", V. Teresa Michel 11, 15121, Italy

suspension, which was then stirred at 50 °C for 20 h. After this time, the sample was filtered and the powder was washed with toluene and ethyl ether to remove the unreacted silane. The obtained sample will be hereafter named NH_2_F5.

Part of this sample was dispersed in 50 mL of HCl (pH 4.0) for 3 h under stirring aiming at promoting the formation of surface NH_3^+ species. The suspension was finally filtered and dried in an oven at 60 °C overnight. The obtained sample will be hereafter named NH_3^+_F5.

2.2 Characterization techniques

Solid state NMR spectra were acquired on a Bruker Avance III 500 spectrometer and a wide bore 11.7 Tesla magnet with operational frequencies for ^{29}Si of 99.35 MHz. A 4 mm triple resonance probe with MAS was employed in all the experiments and the samples were packed on a Zirconia rotor and spun at different MAS rates. The ^{29}Si MAS NMR spectra were recorded under cross-polarization conditions (CPMAS). All chemical shifts are reported using the δ scale and are externally referenced to TMS at 0 ppm.

Thermogravimetric analysis (TGA) was performed on a Setaram SETSYS Evolution instrument under O_2 (gas flow 100 mL min^{-1}), heating the samples up to 800 °C with a rate of 5 °C min^{-1}.

N_2 physisorption measurements were carried out at 77 K in the relative pressure range from 10^{-6} to 1 P/P_0 using a Quantachrome Autosorb 1MP/TCD instrument. Before the analysis the samples were outgassed (residual pressure $p < 10^{-6}$ Torr) at 473 K for 3 h. Specific surface areas were determined by using the Brunauer–Emmett–Teller equation, in the residual pressure range from 0.01 to 0.1 P/P_0. Pore size distributions were obtained by applying the Non-Localized Density Functional Theory (NLDFT) method (N_2 silica kernel based on a cylindrical pore model).

Infrared spectra were collected on a Thermo Electron Corporation FT Nicolet 5700 Spectrometer (resolution 4 cm^{-1}). Self-supporting pellets were placed into an IR cell with KBr windows being permanently connected to a vacuum line (residual pressure: 1.33×10^{-4} Pa, 1 Pa = 0.01 mbar), allowing all treatments and adsorption–desorption experiments to be carried out *in situ*. Before the analysis, samples were outgassed in a vacuum at r.t. for 1 h.

The Zeta potential of silica F5 samples was evaluated with a Zetasizer NANO ZS (Malvern Instruments). Before the analysis the silica samples were dispersed in ultrapure water (2 mg mL^{-1}) and the dispersions were sonicated for 10 minutes.

2.3 Solar cell fabrication

Photovoltaic experiments were performed using 3-{6-{4-[bis(2′,4′-dihexyloxybiphenyl-4-yl)amino-]phenyl}-4,4-dihexyl-cyclopenta-[2,1-*b*:3,4-*b*′]-dithiophene-2-yl}-2-cyanoacrylic acid as a sensitizer, coded Y123, which is described in Fig. 1.

The TiO_2 was deposited on a NSG 10 Glass FTO-coated by screen-printing. We used a spot shaped (area is 0.282 cm^2) transparent TiO_2 layer of 6 μm thickness. The pore size was 32 nm and the TiO_2 particle sizes were equal to 23 nm. $TiCl_4$ treatments were done before and after the transparent TiO_2 film deposition. A platinized FTO conducting glass (LOF TECH 7, Pilkington) was used as the counter electrode. The ionic liquid electrolyte used, coded Z952, is composed of DMII/EMII/EMITCB/I_2/NBB/GNCS (molar ratio: 12/12/16/1.67/3.33/0.67).[24] The gel was prepared by stirring 15% of each kind of particles in the ionic liquid electrolyte overnight. The gel is deposited before sealing and all the cells were doubly sealed once with 25 μm Surlyn and then with Torseal to be sure of the water tightness. For each condition more than 3 cells were made in order to obtain reliable results.

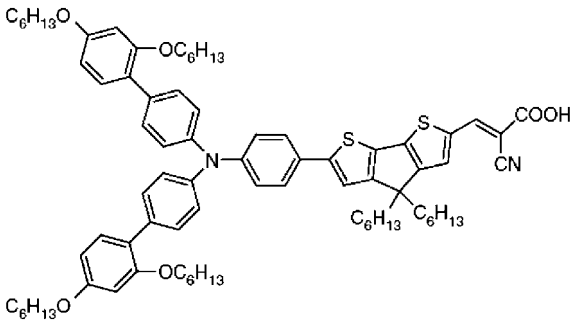

Fig. 1 Structure of the Y123 dye.

2.4 Photovoltaic measurements

The setup used for standard photovoltaic characterization (*J–V* curve) consists of a 450 W xenon lamp (Oriel), whose spectral output was matched in the region of 350–750 nm with the aid of a Schott K113 Tempax sunlight filter (PräzisionsGlas & Optik GmbH), and a source meter (Keithley 2400) to apply a potential bias and measure the photogenerated current. A set of metal-mesh filters was used to adjust the light intensity to a desired level. IPCE was measured using a SR830 lock-in amplifier, however the incident light (300 W xenon lamp, ILC Technology) was focused through a Gemini-180 double monochromator (Jobin-Yvon Ltd). The cells were measured with an external light bias (100 W m^{-2} intensity) provided by LED array. A black metal mask defined the cell active area to be 0.159 cm^2.

Results and discussion

Silica particle modification

A schematic illustration of the process for the modification of silica particles is presented in Fig. 2. In this study commercial bare silica F5 particles and modified silica F5 by NH_2 and NH_3^+ groups were used.

The IR spectrum of the silica F5 sample (Fig. 3A, curve a) is characterized by the presence of a signal located at 3745 cm^{-1} and a broad band with the maximum located at 3500 cm^{-1}. The band at 3745 cm^{-1} is due to the stretching mode of isolated silanols, while the absorption at 3500 cm^{-1} is due to the stretching mode of –OH groups interacting with each other by H-bonding and with the water molecules adsorbed on the surface of the silica. In the low frequency region, the spectrum of the silica F5 sample shows three absorption bands located at

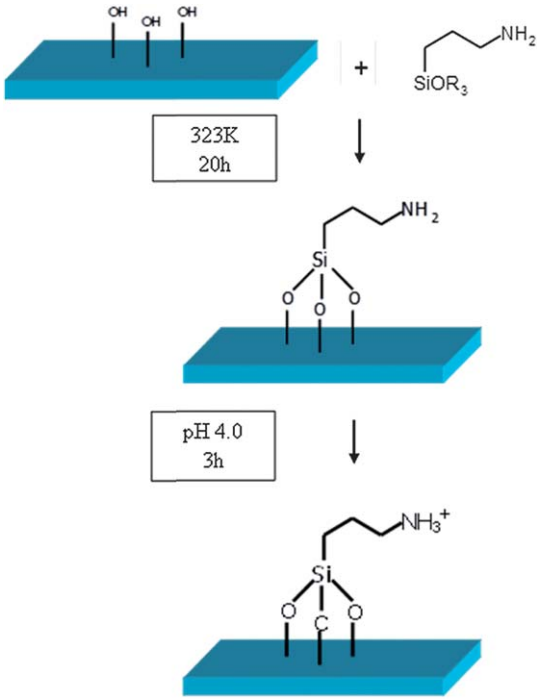

Fig. 2 Schematic representation of silica F5 functionalization with 3-aminopropyltriethoxysilane and formation of NH_3^+ species.

1980 and 1865 cm^{-1}, due to the overtones and combination modes of the silica framework, and at 1655 cm^{-1} due to the presence of water that was not completely removed from the surface of silica during degassing.

The IR spectrum of F5 silica functionalized with 3-aminopropyltriethoxysilane (Fig. 3A, curve b) is characterized by the presence of a broad band in the 3800–3000 cm^{-1} region, in which bands at 3365, 3300, 2940 and 2875 cm^{-1} are visible. In the region at low frequencies other bands at 1600, 1460 and 1445 cm^{-1} are present. The absorptions at 3300 and 2935 cm^{-1} are due to the asymmetric and symmetric stretching modes of NH_2 groups, respectively, whereas the bands at 2940 and 2875 cm^{-1} are assigned due to the asymmetric and symmetric stretching modes of silane $-CH_2$ groups introduced onto the silica surface by an anchoring procedure. The absorption bands in the low frequency region can be assigned to the bending modes of NH_2 groups (1600 cm^{-1}) and to the bending modes of CH_2 groups (bands located at 1460 and 1445 cm^{-1}).

The IR spectrum of the NH_3^+_F5 sample (Fig. 3A, curve c) shows some differences with respect to the spectrum of the NH_2_F5 sample. In particular, the formation of two bands at 1615 and 1505 cm^{-1}, due to asymmetric and symmetric bending modes of NH_3^+ groups, respectively, indicates the formation of surface NH_3^+ species after the treatment under acidic pH (see Fig. 3B).[25]

The Zeta potential of the silica particles and their modified structures are presented in Table 1. The pure silica F5 shows a negative *Z*-potential of *ca.* −18.9 mV due to the presence of SiO^- species on the silica surface. After the reaction with 3-aminopropyltriethoxysilane, the *Z*-potential becomes neutral (*ca.* +3.4 mV), because of the condensation of ethoxy groups of the silane with the hydroxyl groups of the silica surface, while the *Z*-potential of the protonated sample is +29.2 mV, thus confirming the protonation of amino groups on the silica surface.

Thermogravimetric (TGA) analysis of the F5 silica sample (Fig. 4, curve a) showed a weight loss of *ca.* 7% in the 35–150 °C range with a maximum around 85 °C due to removal of adsorbed water. The thermal profile of the NH_2_F5 sample (Fig. 4, curve b) showed three weight losses, the first one of *ca.* 3 wt% in the 35–120 °C range with a maximum at *ca.* 80 °C due to removal of adsorbed water, the second one of *ca.* 4.8 wt% in the 250–420 °C temperature range ascribed to the first decomposition step of 3-aminopropyltriethoxysilane and the third one of *ca.* 5.8 wt% in the 430–630 °C range, with a maximum at *ca.* 560 °C due to the complete removal of organic species from the silica surface. TGA

Table 1 Zeta potential values of F5 silica and organo-modified samples

Sample	*Z* potential [mV]
Silica F5	−18.9 ± 0.29
NH_2_F5	+3.4 ± 0.23
NH_3^+_F5	+29.2 ± 0.54

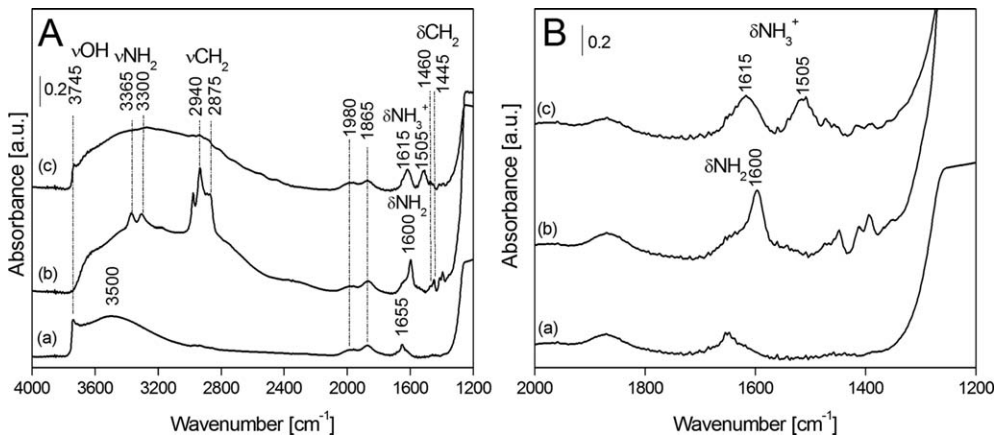

Fig. 3 Frame (A) shows FTIR spectra of F5 silica (curve a) and the sample functionalized with 3-aminopropyltriethoxysilane, before (curve b) and after (curve c) acid treatment at pH 4.0. Frame (B) shows an enlarged view of the FTIR spectra in the 2000–1200 cm^{-1} range. Spectra were recorded after outgassing at room temperature for 1 h.

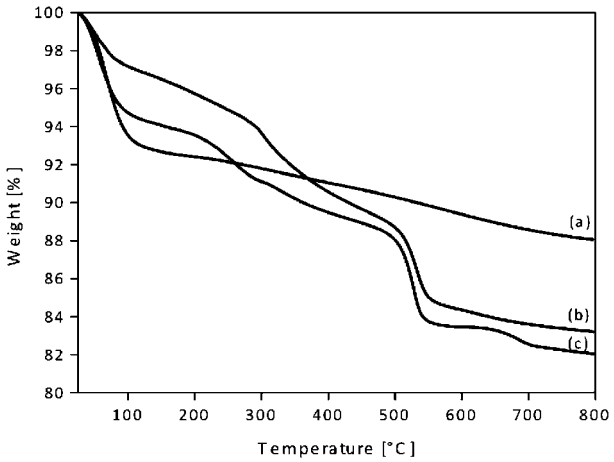

Fig. 4 TGA analysis of F5 silica (a), NH_2_F5 (b) and NH_3^+_F5 (c) samples. The TGA analysis was performed under O_2 flow (100 mL min^{-1}) and using a heating ramp 5 °C min^{-1}.

data indicated that the anchoring procedure allowed introducing *ca.* 11 wt% of organic groups on the surface of F5 silica.

The thermal profile of the NH_3^+_F5 sample (Fig. 4, curve c) showed three weight losses, the first one of *ca.* 6 wt% in the 35–130 °C range with a maximum at *ca.* 70 °C due to removal of adsorbed water, the second one of *ca.* 4.7 wt% in the 165–425 °C range, with two maxima at *ca.* 260 °C and 335 °C ascribed to the decomposition of 3-ammoniumpropyltriethoxysilane and the third one of *ca.* 5.8 wt% in the 440–610 °C range, due to the complete removal of organic species. NH_3^+_F5 silica contains *ca.* 10.5 wt% of organic species. TGA data indicated that the treatment under acidic conditions of NH_3^+_F5 silica does not alter significantly the total amount of organic species anchored onto the silica surface.

The effect of organic functionalization on the textural features of F5 silica was investigated by N_2 physisorption analysis. N_2 adsorption isotherms (frame A) and pore size distribution (frame B) of F5, NH_2_F5 and NH_3^+_F5 samples are reported in Fig. 5.

The adsorption isotherms of the three samples are of type IV based on the IUPAC (International Union of Pure and Applied Chemistry) classification, indicating the presence of mesoporosity in the materials and H_2 hysteresis loop, typical of the presence of disordered pores whose shape is not well defined (Fig. 5A).[26]

The BET algorithm has been used to estimate the specific surface area (SSA) of the solids: parent F5 silica shows a SSA of 630 $m^2 g^{-1}$, whereas the grafted sample has a SSA of 350 $m^2 g^{-1}$. After the treatment under acidic conditions the sample has a SSA of 325 $m^2 g^{-1}$.

The reduction of specific surface area should be ascribed to a modification of the sample surface occurring during the anchoring procedure. The pore size distribution of silica samples was determined by the NLDFT model using the desorption branch of the isotherms (Fig. 5B). The silica F5 sample is characterized by pores with dimensions in the 30–150 Å range. After surface modification and acid treatment, a significant decrease of pore volume is observed, together with the disappearance of small pores in the 30–50 nm range. This is particularly evident for the acid treated sample, NH_3^+_F5.

The result of the reaction between the surface of F5 silica and the silane species was evaluated by solid state NMR spectroscopy. The ^{29}Si CPMAS NMR spectra of the F5 silica sample and NH_2_F5 sample are shown in Fig. 6.

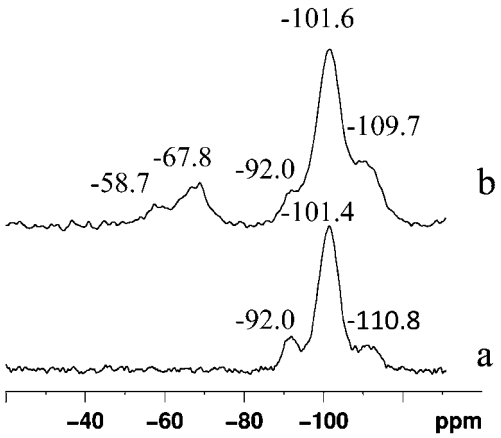

Fig. 6 ^{29}Si CPMAS NMR of silica F5 (curve a) and NH_2_F5 samples (curve b).

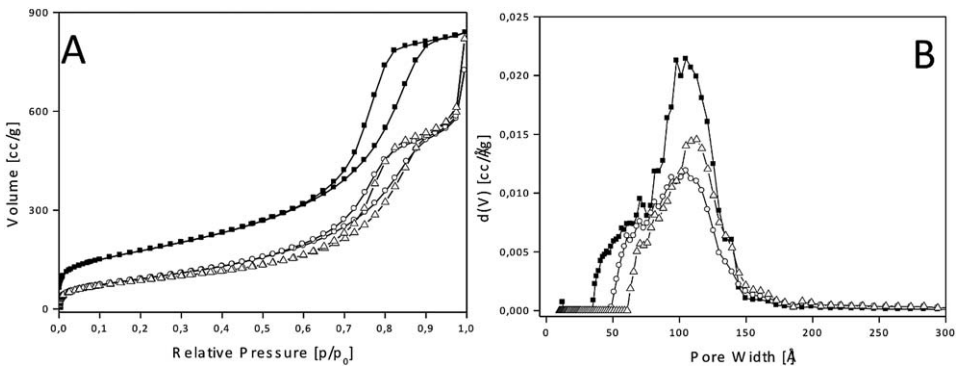

Fig. 5 N_2 adsorption–desorption isotherms at 77 K and relative pressures (P/P_0) from 1×10^{-6} to 1 (A) and pore size distribution determined by NLDFT methods (B) of F5 silica (-■-), NH_2_F5 (-○-) and NH_3^+_F5 (-Δ-) samples.

The spectrum of the F5 silica sample (Fig. 6, curve a) is characterized by the presence of three signals at −92.0, −101.4 and −110.8 ppm that are assigned to Q^2 [$Si(OSi)_2(OH)_2$], Q^3 [$Si(OSi)_3(OH)$] and Q^4 [$Si(OSi)_4$] silicon sites, respectively. The ^{29}Si CPMAS NMR spectra of the NH_2_F5 sample show additional peaks at −58.7 ppm and at −67.8 ppm which are related to T^2 [$Si(OSi)_2(OH)(C)$] and T^3 [$Si(OSi)_3(C)$] species, respectively.[27]

The presence of these signals indicated that silane species are chemically anchored onto the silica surface. In particular, the formation of a large amount of T^3 species with respect to T^2 suggested that the silane is covalently bound to the surface through alkoxide species.

Photovoltaic performance

Following the detailed preparation and characterization of the modified silica particles, each type of modified silica sample was used for the preparation of gel electrolytes. The gels were prepared by stirring 15 wt% of silica sample in the ionic liquid electrolyte overnight. The gel electrolytes were employed in dye sensitized solar cells (further details can be found in the Experimental section).

Fig. 7A shows the *J–V* curves of the DSSCs made from the gel electrolytes. It can be observed that the NH_2_F5 sample gave the highest V_{oc}, around 115 mV higher than the non-modified silica particles (silica F5) and 62 mV higher than the ionic liquid electrolyte. On the other hand the current density and the fill factor are similar for the modified silica particle and pure ionic liquid electrolyte based devices. The highest efficiency of 7.04% under 1 sun illumination was achieved by using the NH_2_F5 gel electrolyte. The incident photon to current efficiency (IPCE) of all the devices is presented in Fig. 7B. Since the current density is similar for the samples the IPCE curves are similar as well and correspond to the Y123 dye spectrum.

The enhancement in the V_{oc} can be related to the change in the pH, as can be seen in Table 2. As the environment becomes less acidic the conduction band of the TiO_2 shifts upward and hence the V_{oc} increases. An additional reason for the enhancement in V_{oc} can be explained by the dark current measurements of the devices containing the NH_2_F5, NH_3^+_F5 and ionic liquid electrolytes (Fig. 8).

The dark current of the NH_2_F5 device is smaller than those of NH_3^+_F5 and the pure ionic liquid electrolyte based devices. The smaller dark current suggests a lower rate of recombination, resulting in an increase of V_{oc}, which is in agreement with our results. These results suggest that the NH_2_F5 gel electrolyte forms a blocking layer, which inhibits the back reaction between the TiO_2 and the electrolyte.

The next step was the determination of the optimal concentration of our best sample (NH_2_F5) in the ionic liquid. Three different concentrations (10 wt%, 15 wt% and 20 wt%) were used in preparing the gel electrolytes (Table 3). Fig. 9 presents V_{oc} as a

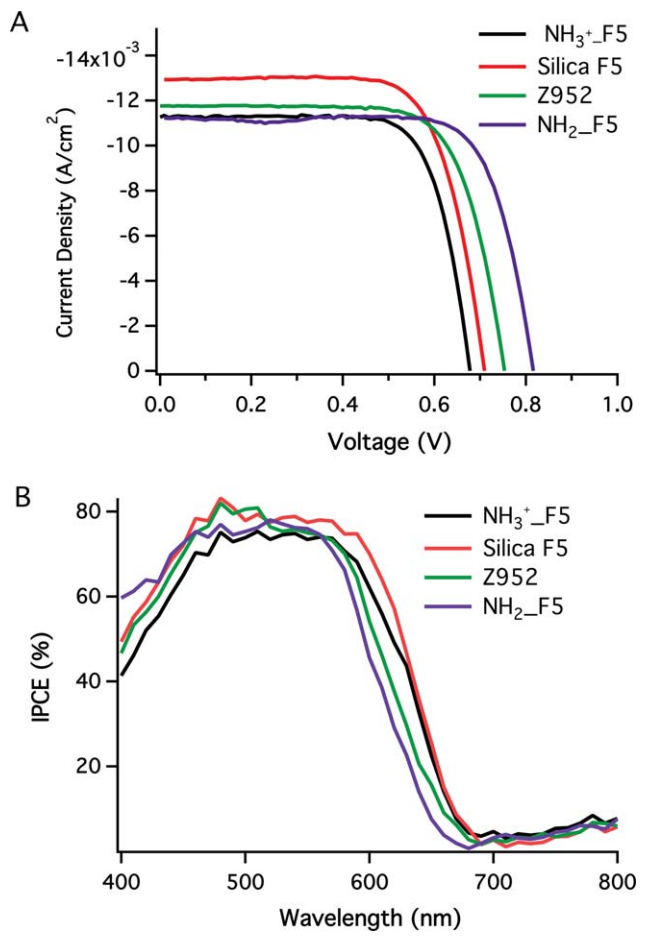

Fig. 7 (A) *J–V* curves of the devices containing gel electrolytes; (B) IPCE spectra of the devices containing gel electrolytes. The gel electrolyte was prepared by adding 15 wt% of modified silica particles in an ionic liquid.

Table 2 Photovoltaic results obtained with various gel electrolytes

	Silica F5	NH_3^+_F5	NH_2_F5	Z952 (ionic liquid)
Efficiency η (%)	6.58	5.84	7.04	6.42
V_{oc} (mV)	699.3	687.4	815.8	753.1
J_{sc} (mA cm^{-2})	12.93	11.31	11.23	11.76
Fill factor	0.72	0.74	0.75	0.72
pH	8.01	6.74	8.65	7.10

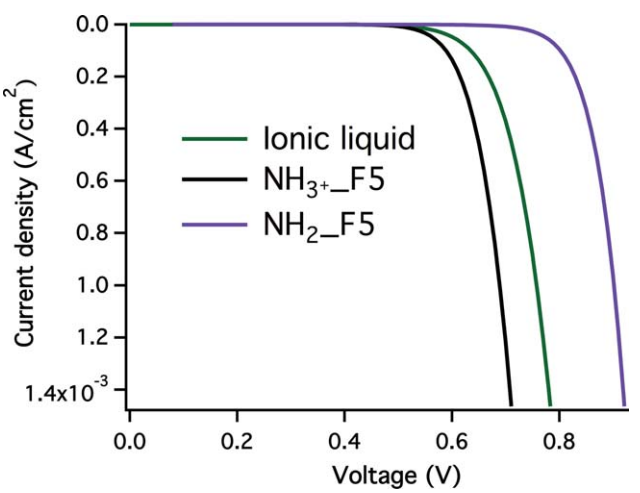

Fig. 8 Dark current measurements of the studied samples.

Table 3 The photovoltaic parameters for different NH_2_F5 concentrations in the ionic liquid electrolyte

NH_2_F5 weight concentration	0%	10%	15%	20%
Efficiency η (%)	6.42	6.2	7.04	5.51
V_{oc} (mV)	753.1	787.1	815.84	805.17
J_{sc} (mA cm^{-2})	11.76	10.45	11.23	9.50
Fill factor	0.72	0.74	0.75	0.71

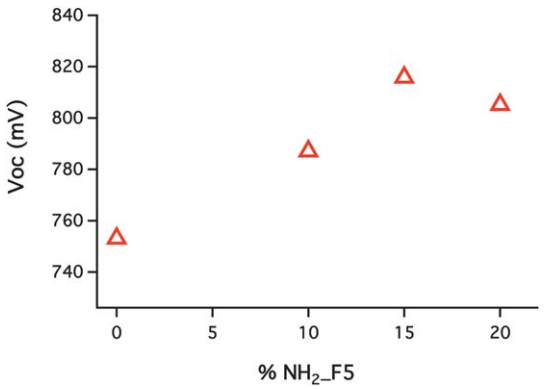

Fig. 9 The change in the V_{oc} of the NH_2_F5 gel as a function of concentration in the ionic liquid electrolyte.

function of the NH_2_F5 concentration; the DSSC device V_{oc} reached its maximum value at 15% concentration. It seems that in the case of 20 wt% concentration the pH of the gel electrolyte is basic which results in the increase of V_{oc} (as explained earlier). But on the other hand the gel electrolyte became very viscous (at 20 wt%) and created a charge transport problem, which inhibited the charge transfer between the dye and the electrolyte. At 10 wt% the pH of the gel electrolyte is not basic as in the case of 15 wt% and 20 wt%, therefore the upward shift of the TiO_2 conduction band is less than in the case of 15 wt%.

Conclusions

Modified silica nanoparticles were used for gelifying an ionic liquid electrolyte to study their influence on the DSSC device performance. It was observed that the modification of the ionic liquid electrolyte by silica particles influences the V_{oc} due to change in the pH and decreased dark current. These modified silica particles offer the possibility to tune the V_{oc} of DSSCs and in addition they will enable the fabrication of solid-state DSSCs that are free of leakage without sacrificing the cell performance. The NH_2 modified silica particles enhanced the device V_{oc} by 62 mV, resulting in 7.04% efficiency at AM 1.5 sunlight.

Acknowledgements

This research was funded by the European Community's Seventh Framework Programme (FP7/2007–2013) under grant agreement no. 227057, Project "INNOVASOL".

References

1 L. M. Peter, *J. Phys. Chem. Lett.*, 2011, **2**, 1861–1867.
2 B. O'Regan and M. Grätzel, *Nature*, 1991, **353**, 737.
3 M. K. Nazeeruddin, A. Kay, I. Rodicio, R. Humphry-Baker, E. Mueller, P. Liska, N. Vlachopoulos and M. Graätzel, *J. Am. Chem. Soc.*, 1993, **115**, 6382.
4 M. Matsumoto, Y. Wada, T. Kitamura, K. Shigaki, T. Inoue, M. Ikeda and S. Yanagida, *Bull. Chem. Soc. Jpn.*, 2001, **74**, 387.
5 F. Cao, G. Oskam and P. C. Searson, *J. Phys. Chem.*, 1995, **99**, 17071.
6 J. Shi, L. Wang, Y. Liang, S. Peng, F. Cheng and J. Chen, *J. Phys. Chem. C*, 2010, **114**, 6814–6821.
7 P. Wang, S. M. Zakeeruddin, J. E. Moser, M. K. Nazeeruddin, T. Sekiguchi and M. Grätzel, *Nat. Mater.*, 2003, **2**, 402–407.
8 B. O'Regan and D. T. Schwartz, *Chem. Mater.*, 1995, **7**, 1349.
9 K. Tennakone, G. R. R. A. Kumara, A. R. Kumarashinghe, I. R. M. Kottegoda, K. G. U. Wijayantha and V. P. S. Perera, *J. Phys. D: Appl. Phys.*, 1998, **31**, 1492.
10 G. R. A. Kumara, S. Kaneko, M. Okuya and K. Tennakone, *Langmuir*, 2002, **18**, 10493–10495.
11 K. Tennakone, G. R. R. A. Kumara, A. R. Kumarsinghe, K. G. U. Wijayantha and P. M. Sirimanne, *Semicond. Sci. Technol.*, 1995, **10**, 1689.
12 U. Bach, D. Lupo, P. Comte, J. E. Moser, F. Weissortel, J. Salbeck, H. Spreitzer and M. Grätzel, *Nature*, 1998, **395**, 583–585.
13 P. Terech and R. G. Weiss, *Chem. Rev.*, 1997, **97**, 3133.
14 S. Yanagida, S. Kambe, W. Kubo, K. Murakoshi, Y. Wada and T. Kitamura, *Z. Phys. Chem.*, 1999, **212**, 31.
15 J. Kruger, R. Plass, L. Cevey, M. Piccirelli, M. Grätzel and U. Bach, *Appl. Phys. Lett.*, 2001, **79**, 2085–2087.
16 M. Boucharef, C. Di Bin, M. S. Boumaza, M. Colas, H. J. Snaith, B. Ratier and J. Bouclé, *Nanotechnology*, 2010, **21**, 205203.
17 T. Katakabe, R. Kawano and M. Watanabe, *Electrochem. Solid-State Lett.*, 2007, **10**, F23.
18 W. Kubo, T. Kitamura, K. Hanabusa and S. Yanagida, *Chem. Commun.*, 2002, 374.
19 N. Mohmeyer, P. Wang, H. W. Schmidt, S. M. Zakeeruddin and M. Gratzel, *J. Mater. Chem.*, 2004, **14**, 1905.
20 E. Stathatos, P. Lianos, A. S. Vuk and B. Orel, *Adv. Funct. Mater.*, 2004, **14**, 45.
21 P. Wang, S. M. Zakeeruddin, P. Comte, I. Exnar and M. Grätzel, *J. Am. Chem. Soc.*, 2003, **125**, 1166–1167.
22 P. Wang, S. M. Zakeeruddin and M. Grätzel, *J. Fluorine Chem.*, 2004, **125**, 1241–1245.
23 C. W. Tu, K. Y. Liu, A. T. Chien, M. H. Yen, T. H. Weng, K. C. Ho and K. F. Lin, *J. Polym. Sci., Part A: Polym. Chem.*, 2008, **46**, 47.
24 Yu. Bai, *et al.*, *Nature Mater.*, 2008, **7**, 626.
25 Von N. B. Colthup, L. H. Daly and S. E. Wiberley, *Introduction to Infrared and Raman Spectroscopy*, Academic Press, Boston, MA, 3rd edn, 1990.
26 S. Lowell, J. E. Shields, M. A. Thomas, M. Thommes, *Characterization of Porous Solids and Powders: Surface Area, Pore Size and Density*, Kluwer Academic Publishers, 2004.
27 S. H. Kim, O. C. Han, J. K. Kim and K. H. Lee, *Bull. Korean Chem. Soc.*, 2011, **32**(10), 3644.